Medical Physics
The International Journal of Medical Physics Research and Practice

Characterization of optically stimulated luminescent dosimeters, OSLDs, for clinical dosimetric measurements

Paul A. Jursinic

Citation: Medical Physics **34**, 4594 (2007); doi: 10.1118/1.2804555
View online: http://dx.doi.org/10.1118/1.2804555
View Table of Contents: http://scitation.aip.org/content/aapm/journal/medphys/34/12?ver=pdfcov
Published by the American Association of Physicists in Medicine

Characterization of optically stimulated luminescent dosimeters, OSLDs, for clinical dosimetric measurements

Paul A. Jursinic[a)]
West Michigan Cancer Center, 200 North Park Street, Kalamazoo, Michigan 49007

(Received 26 April 2007; revised 5 September 2007; accepted for publication 28 September 2007; published 9 November 2007)

Optically stimulated luminescent dosimeters, OSLDs, are plastic disks infused with aluminum oxide doped with carbon (Al_2O_3:C). These disks are encased in a light-tight plastic holder. Crystals of Al_2O_3:C when exposed to ionizing radiation store energy that is released as luminescence (420 nm) when the OSLD is illuminated with stimulation light (540 nm). The intensity of the luminescence depends on the dose absorbed by the OSLD and the intensity of the stimulation light. OSLDs used in this work were InLight/OSL Dot dosimeters, which were read with a MicroStar reader (Landauer, Inc., Glenwood, IL). The following are dosimetric properties of the OSLD that were determined: After a single irradiation, repeated readings cause the signal to decrease by 0.05% per reading; the signal could be discharged by greater than 98% by illuminating them for more than 45 s with a 150 W tungsten-halogen light; after irradiation there was a transient signal that decayed with a 0.8 min halftime; after the transient signal decay the signal was stable for days; repeated irradiations and readings of an individual OSLD gave a signal with a coefficient of variation of 0.6%; the dose sensitivity of OSLDs from a batch of detectors has a coefficient of variation of 0.9%, response was linear with absorbed dose over a test range of 1–300 cGy; above 300 cGy a small supra-linear behavior occurs; there was no dose-per-pulse dependence over a 388-fold range; there was no dependence on radiation energy or mode for 6 and 15 MV x rays and 6–20 MeV electrons; for Ir-192 gamma rays OSLD had 6% higher sensitivity; the dose sensitivity was unchanged up to an accumulated dose of 20 Gy and thereafter decreased by 4% per 10 Gy of additional accumulated dose; dose sensitivity was not dependent on the angle of incidence of radiation; the OSLD in its light-tight case has an intrinsic buildup of 0.04 g/cm^2; dose sensitivity of the OSLD was not dependent on temperature at the time of irradiation in the range of 10–40 °C. The clinical use of OSLDs for *in vivo* dosimetric measurements is shown to be feasible. © *2007 American Association of Physicists in Medicine*. [DOI: 10.1118/1.2804555]

Key words: optically stimulated luminescent dosimeters, *in vivo* dosimetry, thermoluminescent dosimeters, diodes

I. INTRODUCTION

Radiation treatments of cancer patients require deliveries of high dose, usually 180 cGy or more per day, for 30–40 consecutive daily treatments. *In vivo* dosimetry is desired for cancer patients to ensure that the patient is not overexposed or that the exposure occurred in the desired region.[1] *In vivo* dosimetry has traditionally been provided by thermoluminescent dosimeters,[2] TLDs, *PN*-junction-type diodes,[3] or metal-organic semiconductor field-effect transistor (MOSFET) detectors.[4]

The first use of optically stimulated luminescence, OSL, as a dosimeter was to measure luminescence from quartz for dating sediments and artifacts from archeological samples[5–7] exposed to background radiation for thousands of years. The use of synthetic materials for OSL (Ref. 8) has greatly improved the sensitivity of the method; it has now been used for about 10 years[9] as a method for monitoring occupational radiation dose. OSL dosimeters have been a replacement for personnel dose monitoring with film badges. The OSL material has now been fabricated into a dosimeter that can be used for *in vivo* dosimetry of radiation therapy patients.

The phenomenological description of the OSL, and thermoluminescence, TL, process are the same.[2,10] Pure crystalline dielectric materials either contain or have added trace amounts of contaminants that form crystal-lattice imperfections. These imperfections act as traps for electrons or holes and also can act as luminescence centers, which emit light when electrons or holes recombine near them. This process is shown schematically in Fig. 1, based on energy-band schemes previously published.[11–14] After irradiation, free electrons and holes are generated that can be trapped. The dosimetric trap, 4 in Fig. 1, is associated with a thermoluminescent, TL, peak at 180 °C (Ref. 13) and can store electrons at ambient temperature for over 100 days.[15] The recombination centers in Al_2O_3:C are mainly created by oxygen vacancies and are called F centers[8] (5 and 11 in Fig. 1). Radiation generated holes can be trapped at the recombination center, creating F^+ centers. When the crystal is heated or optically stimulated, electrons can be ejected out of traps (9 in Fig. 1) and recombine with holes at the $F+$ center (11 in Fig. 1). The recombination energy is transferred to a luminescence center where light is emitted; $F^+ + \text{electron} \rightarrow F + 420$ nm light[8] (12 Fig. 1). If this recombination cascade is

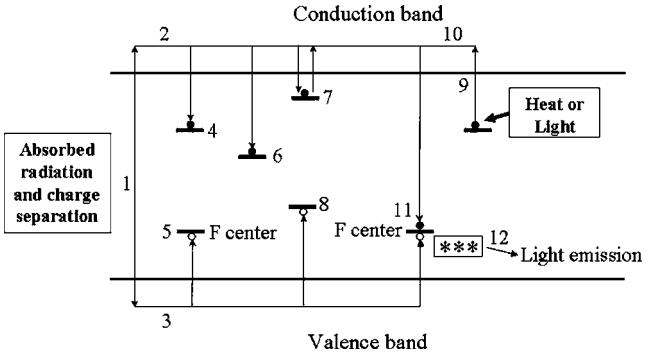

FIG. 1. A schematic diagram of the energy levels of a crystalline material that sustains thermoluminescence or optical luminescence. The numbers in the diagram represent the following: 1 is the absorption of radiation and subsequent charge separation; 2 is the migration and trapping of an electron, ●, after charge separation; 3 is the migration and trapping of an hole, ○, after charge separation; 4 is a moderately deep electron trap; 5 is a moderately deep hole trap; 6 is a very deep electron trap; 7 is a shallow electron trap; 8 is the ejection of an electron out of a trap by absorption of heat, thermoluminescence, or light, optical luminescence; 9 is the migration of the untrapped electron; 10 is the recombination of an electron and hole at a hole trap; 11 is the emission of light at a luminescence center, ***, which received energy from the recombination of the electron and hole.

initiated by heat then it is called thermoluminescence; if it is initiated by light then it is called optically stimulated luminescence. Dosimetric traps are energetically deep enough to hold charge at room temperature for long periods of time, but are not so deep that the charge cannot be released by illumination with visible light.[16] Besides dosimetric traps there are shallow electron traps (7 in Fig. 1) which are unstable at ambient temperature and hold charge for only a few seconds or minutes even without optical stimulation. Deep electron traps (6 in Fig. 1) also exist with a TL peak at 700–1000 °C (Ref. 13) and will release trapped charge only at very high temperatures or with optical stimulation with ultraviolet light.[16] There also are deep hole traps (8 in Fig. 1) that can compete for separated charge.[11,17] For an OSLD the intensity of the luminescence depends on the dose absorbed, numbers of luminescent traps that are filled, and the light intensity of the stimulation light.

Originally Al_2O_3 crystals grown in the presence of carbon were intended to be used as TLDs.[18,19] However, Al_2O_3:C as a TLD had the disadvantage of being discharged by exposure to visible light. This "disadvantage" from the point of view of a TLD was in fact a serendipitous advantage. It was quickly realized that optical discharging gave rise to OSL that was proportional to the dose of ionizing radiation absorbed by the Al_2O_3:C crystal.[8,10,19–22]

OSLD made of Al_2O_3:C can be stimulated with a broad spectrum of light from 400 to 700 nm with a peak at 475 nm.[10,21] The emission occurs in a broad band of wavelengths with a peak centered at 410–420 nm.[8,21] The OSLD can be read out with light in continuous wave, cw, mode[23,24] or with the light in pulsed mode.[10,22,25,26] In the cw mode the stimulation light and the detector are on continually and narrow-band optical filters are used to discriminate between the stimulation and emission light. In the pulsed mode the stimulation light and detector are only active for short periods of time that are asynchronous, so separation of light signals is accomplished temporally.

The OSL afterglow decay curve is composed of two different exponential decay functions. One decay function reported to be both temperature independent[21,25] and temperature dependent[27] with a lifetime of 35 ms and arises from excited *F* centers, *** in Fig. 1. The other decay is temperature dependent with a lifetime from hundreds of milliseconds to seconds.[16,21,25] The temperature-dependent component arises from shallow electron traps, 7 in Fig. 1.

There are two measurement modes that can be invoked for use of OSL as a dosimeter in clinical applications. The first measurement mode, integrating mode,[28] is to expose the OSL dosimeter in a radiation field and at a later time read out the OSL signal that is proportional to the absorbed dose.[13,29–32] The second measurement mode, real-time mode,[28] is readout of the luminescence signal, which is called radioluminescence, during the radiation delivery.[24,29–31,33] The first method, the integrating mode, is characterized and reported in this work. This was the reading method that was used in the commercially available equipment that we had access to in our clinic.

II. MATERIALS AND METHODS

The x-ray beams used in this work had nominal energies of 6 and 15 MV. For these energies, respectively, the percent depth dose of x rays at depth 10 cm, $\%dd(10)_x$, was 66.6 and 77.8, which was measured at source-to-surface distance of 100 cm, according to the TG-51 protocol.[34] The electrons beams used had nominal energies of 6, 9, 12, 16, and 20 MeV, which had depths of 50% maximum dose, R_{50}, of 2.34, 3.61, 5.02, 6.63, and 8.26 cm, respectively. These R_{50} were measured at source-to-surface distance of 100 cm, according to the TG-51 protocol.[34] The x-ray beams were generated by a KD2 linear accelerator (Siemens Medical Systems, Concord, CA) or a Varian Trilogy (Varian Medical Systems, Milpitas, CA) linear accelerator.

Irradiations with Ir-192 were made with a high dose rate (HDR) GammaMed source (Varian Medical Systems, Milpitas, CA). The Ir-192 source and the detectors were separated by 7.1 cm in a stack of solid water and Superflab that was 30 cm^3. Superflab is a flexible water equivalent material (Civco, Orange City, IA). The use of Superflab avoided the need for the slabs of solid water (Standard Imaging, Madison, WI) to be machined for the various detectors. The Superflab and solid water were used for buildup and backscatter material. The dose rate at the detector position was calculated using the TG-43 protocol.[35] The air-kerma strength of the source was measured with a model HDR100Plus well chamber (Standard Imaging, Middleton, WI) that had been calibrated at an Accredited Dosimetry Calibration Laboratory.

Absolute dose measurements were made with a cylindrical ion chamber, model N30001 (PTW, Hicksville, NY), which had been calibrated at the University of Wisconsin Dosimetry Calibration Laboratory. All doses delivered by the

accelerators were compared against ion chamber measurements that were traceable to TG-51 (Ref. 34) calibrations.

Depth dose measurements were made with a parallel-plate ion chamber, Markus N23343 (PTW, Freiburg, Germany). For this ion chamber a 3 cm thick slab of solid water was used that had been machined to fit the chamber with its top surface flush with the top surface of the solid water block.

The diode used in these measurements was a *P*-type semiconductor, surface diode, model 1113000–0 (SunNuclear, Melbourne, FL). This type of diode has an active volume of $1.6\times1.6\times0.05$ mm^3 that is encased in a thin, epoxy housing with an intrinsic buildup of 0.11 g/cm^3. The diode output was measured with a clinic-built amplifier that integrated charge during radiation exposures.

The thermoluminescent dosimeters, TLDs, used in this work were TLD-100 type LiF chips, model SNO 18835 (Thermo Electron Corporation, Santa Fe, NM). This type of TLD is $3.2\times3.2\times0.9$ mm^3. The TLD was read with a model 3500 digitally programmable reader (Harshaw/Thermo Electron Corporation, Santa Fe, NM). The TLDs were read with the following heating cycle: preheat for 10 s at 100 °C, read for a 20 s ramp from 100 to 300 °C, and an annealing step of 10 s at 300 °C. The preheat step depleted all low-energy traps (7 in Fig. 1) before the reading of the TLD. The annealing step reduced residual signals to less than 0.2%. This reading and heating cycle allowed TLDs to be read repeatedly with a turnaround time of approximately 1 min. With careful calibration of each individual TLD, repeated readings can be made with a coefficient of variation of 1.5%.

The OSLDs that were used were InLight/OSL Dot dosimeters (Landauer, Inc., Glenwood, IL). The OSLDs are 7 mm diameter, 0.2 mm thick plastic disks infused with aluminum oxide doped with carbon (Al_2O_3:C), synthetic sapphire. These disks are encased in a $24\times12\times2$ mm^3 light-tight plastic holder. The plastic has a mass density of 1.03 g/cm^3 and the plastic leaves that cover the front and back of the OSLD disk are 0.36 mm thick. This gives an areal density of the covering of the OSLD disk of 0.037 g/cm^2.

OSLDs were read with an InLight microStar reader (Landauer, Inc., Glenwood, IL). This reader operates in cw mode with a 1 s illumination-read period. The reader was operated in its "Hardware Test" modality, using the low-intensity LED beam for pre- and post-irradiation measurements. The low-intensity LED mode was used because the OSLD light signal from 200 cGy was found to saturate the optical detector circuits when the high-intensity LED mode was used. The optical detector circuits were found to begin to saturate whenever the counts exceeded about 1.6×10^6. The readout light is provided by a model NSPG500S LED (Nichia, Inc. Tokyo). The LED passes through a color glass bandpass filter OG515 (Melles Griot, Rochester, NY). This LED-filter combination has a peak emission at 540 nm.

The OSLD signal was read directly by a photomultiplier filtered with a color glass bandpass filter B370 (Hoya, San Jose, CA). This photomultiplier-filter combination has peak sensitivity at 420 nm. All OSLDs were read before irradiation and reported signals were the difference between the post-irradiation and pre-irradiation signal reported in photomultiplier counts.

TABLE I. Geometric parameters for various modes and energies of the linear accelerator operation that correspond to 1 cGy/MU calibrated according to TG-51 (Ref. 34). The detector was placed at the depth of maximum dose. The depth of the detector was provided by a combination of a 0.5 cm thick piece of Superflab and various pieces of solid water.

Radiation mode	Energy	Field size	Detector depth, cm	SSD, cm
X-ray	6 MV	10×10 cm	1.6	98.4
X-ray	15 MV	10×10 cm	3.0	97.0
Electrons	6 MeV	10 cm cone	1.2	100
Electrons	9 MeV	10 cm cone	2.0	100
Electrons	12 MeV	10 cm cone	2.9	100
Electrons	16 MeV	10 cm cone	3.5	100
Electrons	20 MeV	10 cm cone	2.7	100

The number of pulses produced by the linear accelerator in an irradiation was determined by the pulse counter of a Profiler, a diode linear-array detector (Sun Nuclear, Melbourne, FL). The period of the pulses was determined by dividing the irradiation time by the number of pulses counted. The pulse width was determined by measuring the time duration of the target current with an oscilloscope, model 2247A (Tektronics, Beaverton, OR).

Irradiations of the detectors that were done orthogonal to the front surface had a source-to-detector distance of 100 cm. A 0.5 cm thick piece of Superflab was placed immediately over the detectors, which conformed to the irregular shapes of the detectors without large air gaps. Geometric parameters are given in Table I that correspond to 1 cGy/MU for various modes and energies calibrated according to TG-51.[34] An 8 cm thick block of solid water was placed behind the detectors to provide backscatter of radiation.

For measurements of angular dependence, cylindrical phantoms with 3.6 cm diameter and 5 cm length were fabricated to provide buildup that was homogeneous in all directions. The phantoms were cast from well-stirred, molten material, *M*3,[36,37] which is water equivalent. The cylinders were sawed in half and each hemi-cylinder was carved out at the geometric center to fit an OSLD in its light-tight case, a surface diode, or a TLD. The hemi-cylinders were then reassembled into cylinders and held together with tape. The cylindrical phantom was then mounted on a 20 cm tall block of high-density Styrofoam, which had been marked off in degrees of rotation. The Styrofoam block provided an easy way to set the angular position of the detectors in the cylindrical phantom and to avoid inadvertent scatter from the treatment couch. For these measurements the accelerator gantry was stationary and was set at 90° so that the beam axis was parallel to the floor. A 10×10 cm^2 field size was used. The long axis of the cylindrical phantom was the axis of rotation and it was vertical, which was perpendicular to central axis of the accelerator beam. Zero degrees of rotation corresponded to the front surface of the various detectors.

A bright light source was used to bleach or optically anneal the irradiated OSLDs after they had been read. An endoscopic illuminator, model 481C, miniature cold light fountain (Karl Storz, Los Angeles, CA) was used. This illuminator had a 150 W tungsten-halogen lamp focused onto an optical port. A 4 mm diameter, 30 cm long light guide was attached to the optical port. The light guide focused the light and acted as a heat shield to avoid melting the plastic housing of the OSLD. The optical spectrum of this bleaching light is not known. A plastic fitting was machined that firmly held the OSLD with its case opened at the end of the light guide. OSLDs were bleached a few minutes before irradiation. Also, after bleaching the OSLD signal was measured to determine what level of residual signal remained.

The dose sensitivity of OSLDs and the diode was tested for different temperatures during irradiation. The experimental setup was 4 cm of solid water, a 1 cm thick Styrofoam slab for thermal insulation, the detectors, and a thin plastic water bath whose bottom was in thermal contact with the detectors. The accelerator beam was aimed through the slab of solid water. The temperature of the water bath was adjusted by adding ice or warm water until the desired temperature was attained. Thermal equilibrium with the detectors was established by allowing 5 min at a particular temperature before an irradiation was made.

In these temperature measurements the diode served two functions: a radiation detector and a temperature detector. The temperature of the OSLD and the diode was measured by operating the diode as a thermistor.[38,39] The diode was forward biased with 440 mV of a digital volt-ohm meter operated in the resistance-measurement mode. The resistance of the forward-biased diode was measured with a digital volt-ohm meter, model 77 (Fluke, Everett, WA). The resistance-versus-temperature dependence was measured by letting the diode equilibrate for 5 min to various temperatures in a water bath whose temperature was measured with a laboratory thermometer. After the temperature reading, the diode was connected to the amplifier and used in its second function as a radiation detector.

III. RESULTS

Each reading of an OSLD partially discharges the trapped charges and reduces the OSLD signal. Figure 2 shows the OSLD signal for repeated readings. A linear regression on these data gives an intercept of 0.998, a slope of −0.000 65,

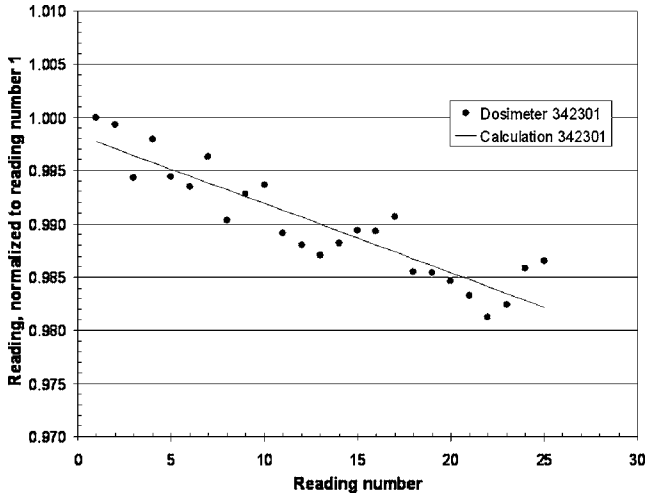

FIG. 2. The depletion of an OSLD optical signal when given sequential readings. The OSLD was exposed to 100 cGy of 6 MV x rays and then kept in the dark for 10 min. After the dark period, the OSLD was read 25 times. The OSLD signals were normalized to value of the first reading. The solid line is a calculation based on Eq. (1) with $f=0.9993$.

and a standard deviation of the residuals of 0.2%. A mathematical model for the signal decrease is the following:

$$S(n) = S(n=0) \cdot f^n, \tag{1}$$

where $S(n)$ is the signal on reading n, $S(n=0)$ is the putative signal before any reading depletion, and f is the fraction by which the signal is depleted per reading. Equation (1) can be made linear as follows:

$$a = 1 - f,$$

$$f^n = (1-a)^n \approx 1 - n \cdot a \quad \text{when} \quad a \ll 1.$$

Substituting into Eq. (1),

$$S(n) = S(n=0) \cdot (1 - a \cdot n) = S(n=0) - S(n=0) \cdot a \cdot n, \tag{2}$$

which is a linear equation with an intercept, $S(n=0)$, and a slope, $-S(n=0) \cdot a$. The measurements shown in Fig. 2 were repeated for two other OSLDs and the analyzed results are presented in Table II. The fraction of decrease in the signal on each reading is different for each OSLD but is approximately 0.9995. Each reading decreases the OSLD signal by 0.05%. The standard error indicates that when reading an

TABLE II. Analysis of the reading depletion for three OSLDs. These OSLDs were irradiated with 100 cGy of 6 MV x rays and were read 25 times sequentially with the low-intensity LED beam. The reading data were analyzed with linear regression, according to Eqs. (1) and (2).

	OSLD #342301	OSLD #34470T	OSLD #34484K
Intercept	0.998 ± 0.0009	0.994 ± 0.0015	1.0033 ± 0.0013
Slope	$-6.5 \times 10^{-4} \pm 6.2 \times 10^{-5}$	$-5.5 \times 10^{-4} \pm 1.0 \times 10^{-4}$	$-2.7 \times 10^{-4} \pm 9.0 \times 10^{-5}$
Standard deviation of the residuals	0.0022	0.0036	0.0032
a [Eq. (2)]	6.5×10^{-4}	5.5×10^{-4}	2.7×10^{-4}
f [Eqs. (1) and (2)]	0.9993	0.9994	0.9997

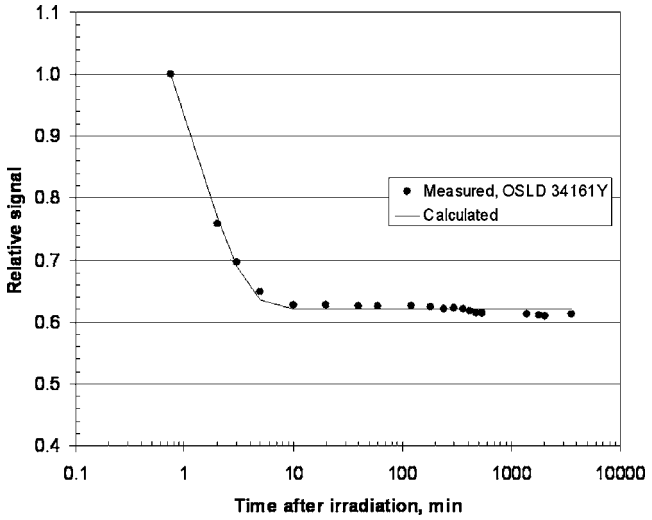

FIG. 3. Repeated measurements of an OSLD vs the time after irradiation. These repeated measurements were corrected for the signal depletion by measurement, using Eq. (1) with $f=0.9995$. OSLDs irradiated with 100 cGy were normalized to the first signal measured. The solid lines are calculations based on Eq. (3) with parameters shown in Table III.

OSLD after a single irradiation an uncertainty of 0.3% is found. This standard error is consistent with the counting statistics of $1/\sqrt{100\,000}$ for 100 000 counts. Equation (1) can be used to correct for signal depletion when multiple sequential readings of an OSLD are carried out.

TLDs have low-temperature traps that are unstable at room temperature and decay away in the dark in a few minutes.[2] It was important to determine if the OSLDs also have unstable traps that might contribute to a transient signal immediately after irradiation. For these measurements the OSLD was irradiated and readings were begun within 45 s after the end of the irradiation. An OSLD was irradiated with 100 cGy and the measured signal is plotted in Fig. 3. Clearly, there is a transient signal, which decays away in a few minutes after irradiation of the OSLD. A mathematical model for the decrease in signal is the following:

$$S(t) = A + B \cdot e^{-kt}, \tag{3}$$

where $S(t)$ is the OSLD signal at time, t, after the irradiation, A and B are constants, and k is the decay constant. The measured data are fit with a nonlinear regression, steepest-descent method. The analysis of the measurements shown in Fig. 3 is presented in Table III. Also shown in Table III is the analysis of the decay of two other OSLDs. The decay parameters are different for each OSLD. However, a wait time in the dark of ten halftimes, approximately 8 min after irradiation, is adequate to avoid this transient signal in all of the OSLDs. There is also a very slow decay of the OSLD signal of about 2% from 10 to 3600 min (2.5 days) after irradiation. For the remaining measurements presented in this work, an 8–15 min wait after the end of an irradiation was allowed before the OSLD signal was read.

OSLDs are normally kept in the dark in their light-tight cases after irradiation. However, it was of interest to determine how the OSLD might be bleached or optically annealed and at what light levels they might be handled when not in their light-tight case. OSLDs were irradiated and then exposed to various light levels for different amounts of time, followed by 3 min of dark before they were read. The dark interval after illumination was needed to avoid interference from phosphorescence of the OSLD. Figure 4 shows the results of these measurements. Illumination with the tungsten-halogen lamp discharges the OSLD by greater than 98% in 45 s, bright room light takes 2 h to discharge the OSLD by about 93%, and in dim room light only 15% of the signal is dissipated in 2 h. In order to optically anneal an OSLD an exposure of 1 min to the tungsten-halogen lamp will be adequate.

TABLE III. Analysis of the decay of the OSLD signal after irradiation for three OSLDs. These OSLDs were irradiated with 6 MV x rays and were read beginning at 45 s after the end of irradiation. Equation (1) was used to correct for signal depletion with these multiple sequential readings of the OSLDs. The reading data were analyzed by nonlinear regression, according to Eq. (3).

	A	B	k min^{-1}	$t_{1/2}=0.693/k$ min
OSLD 34161Y, 100 cGy	0.620	0.664	0.753	0.92
OSLD 342301, 100 cGy	0.642	0.978	1.473	0.47
OSLD 34322W, 100 cGy	0.623	1.016	1.457	0.48

OSLDs can be used with the following procedure: optically bleached, irradiated, and read. This cycle can be repeated many times. This type of repeated measurement was carried out and the sensitivity of the OSLD was measured. These data are shown in Fig. 5 for two different OSLDs. The sensitivity of the OSLDs is unchanged within the reading uncertainty of 0.6% until about 20 Gy of dose is accumulated. Above 20 Gy, the OSLD sensitivity begins to drop by about 4% per 10 Gy of additional accumulated dose.

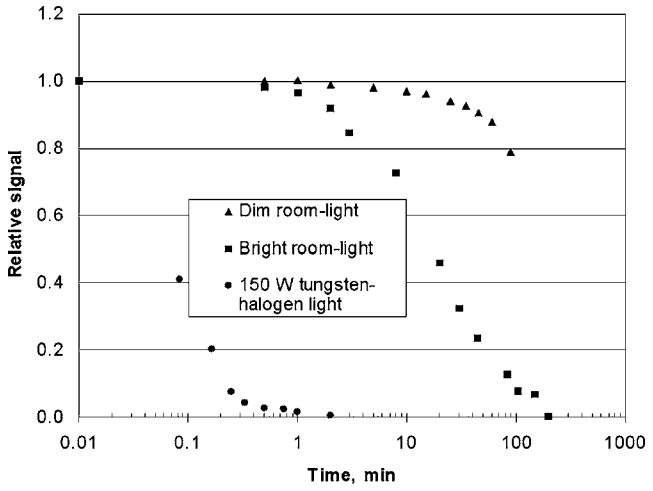

FIG. 4. Measurements of an OSLD signal after various times of optical illumination. The OSLDs were irradiated with 100 cGy of 6 MV x rays and were kept in the dark for 30 min before reading. The OSLDs were then illuminated for the indicated times with a 150 W tungsten-halogen lamp, bright room light that was typical of an office environment, and dim room light that was typical of a linear accelerator environment.

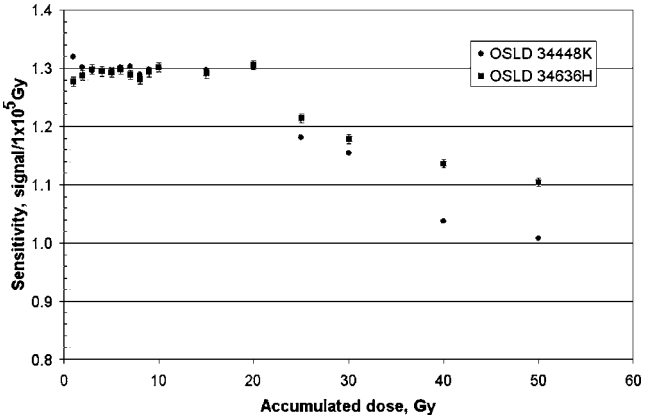

FIG. 5. Sensitivity of OSLDs vs accumulated dose. Two different OSLDs were exposed to different amounts of accumulated dose. The sensitivity of the OSLD was then tested by bleaching, irradiating with 100 cGy of 6 MV x rays, and then reading the OSLD signal after an 8 min wait. The error bars indicate the measurement uncertainty of 0.6% observed for these OSLD measurements.

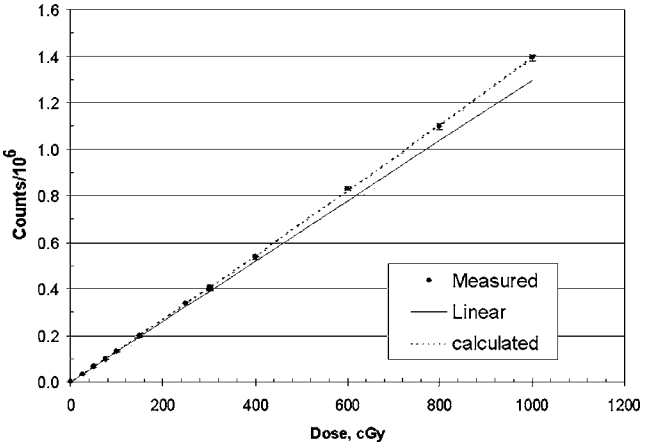

FIG. 6. OSLD response vs absorbed dose. Each dose point is a different OSLD randomly chosen from a batch of OSLDs. The points are measured values with error bars indicating the measurement uncertainty of 0.9% observed for these OSLD measurements. The broken line corresponds to values calculated with Eq. (4). The solid line shows linear dependence on dose based on the response of OSLD data up to 100 cGy.

The stability of OSLD sensitivity for a single detector was tested. A single OSLD was irradiated with 100 cGy of 6 MV x rays, read, and zeroed repeatedly. These data are shown in Table IV and found to have a coefficient of variation of 0.63%.

Another method of use is to obtain OSLDs from a batch of detectors with similar sensitivity. In this case the OSLDs are irradiated, read, and then discarded. To test this method OSLDs were used which had never been irradiated. These dosimeters were not pre-selected but were randomly selected from a batch of dosimeters. The OSLDs were irradiated one time to various doses of 6 MV x rays and these data are shown in Fig. 6. As can be seen, the OSLDs behave like TLDs and exhibit supra-linear response to dose above 300 cGy. The OSLD response is modeled by the following equation:

$$\text{dose(cGy)} = 7.525 \times 10^{-4} \times \text{counts} - 2.541 \times 10^{-11} \times \text{counts}^2, \quad (4)$$

which is shown as the broken line in Fig. 6. This batch of OSLDs had a coefficient of variation of 0.9% for 100 cGy irradiation. The coefficient of variation is based on six different OSLDs shown in Table IV.

The angular dependence of the detectors was determined by irradiating them with 50 cGy of 6 MV x rays collimated into a 10×10 cm^2 field. Figure 7 shows these data for the OSLD, TLD, and surface diode. The OSLD and TLD show no angular dependence within the measurement uncertainty, which is 0.9% for the OSLD and 1.9% for the TLD. The diode has a complicated dependence on the incident angle of

TABLE IV. Exposure data and statistical analysis for one OSLD, 34636H, repeatedly exposed to 100 cGy, read, and then optically annealed. These data for OSLD 34636H are the first six data points in Fig. 5. Data are also shown for six different OSLDs randomly chosen from a batch of detectors.

OSLD 34636H Trial	Net counts	OSLD	Net counts
1	127 667	34 742M	132 632
2	128 773	34 413T	130 315
3	129 799	34 342U	131 809
4	129 428	34 442S	129 265
5	129 281	34 285M	131 859
6	129 757	34 756D	130 851
Average	129 109		131 121
Standard deviation	807		1 222
Coefficient of variation	0.63%		0.93%

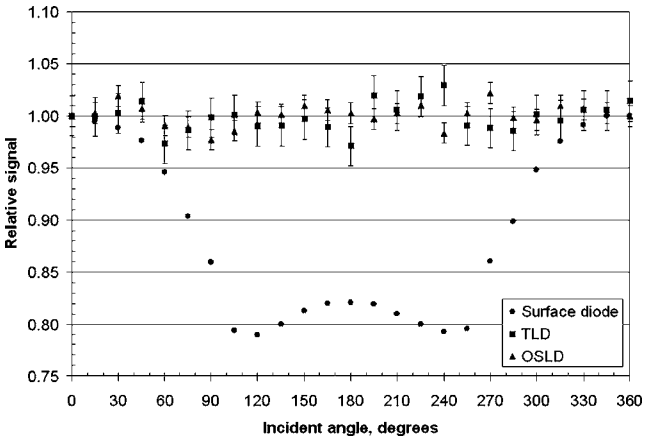

FIG. 7. The radiation sensitivity of an OSLD, a TLD, and a surface diode as a function of the angle of incidence of radiation. The OSLD and TLD were zeroed, irradiated, and read for each incident angle. All signals were normalized to the sensitivity measured at 0°, which was the incident angle of the central axis of the beam when it was perpendicular to the front surface of the detector. The error bars are one standard deviation of measurement error for the OSLD.

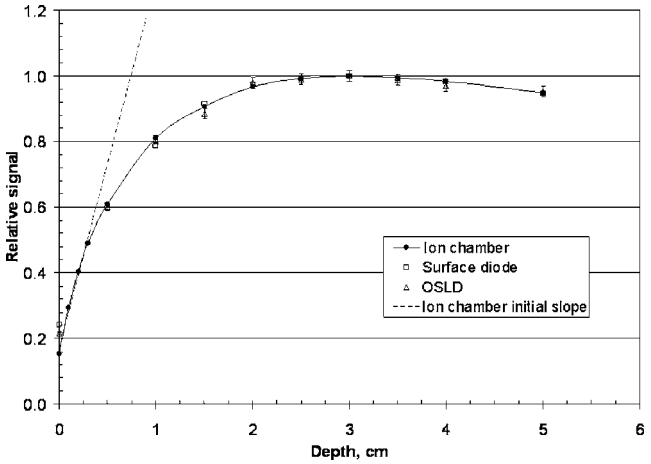

FIG. 8. The depth dose of a 15 MV x-ray beam measured with a parallel-plate ion chamber, an OSLD in its light-tight case, and a surface diode. The source-to-surface distance for these measurements was kept constant at 100 cm. The depth was adjusted by adding pieces of solid water and a 5 mm piece of Superflab directly over the OSLD and the surface diode. All data are normalized to the maximum values at a depth of 3 cm. The broken line is a linear fit to the parallel-plate ion chamber data for depths 0, 1, 2, and 3 mm. The error bars indicate the measurement error of 0.9% observed for these OSLD measurements.

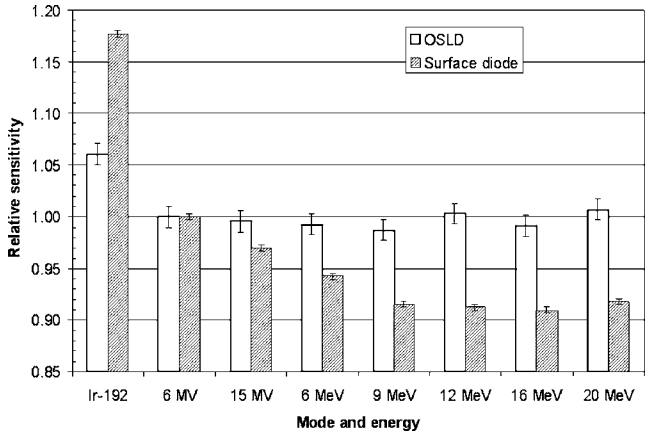

FIG. 9. OSLD and diode sensitivity for various modes and energies of radiation used in the clinic. The detector was positioned at the depth of maximum dose as described in Table I for the linear accelerator irradiation. The Ir-192 source was positioned 7.1 cm away from the detectors. The delivered dose was 100 cGy for all modes and energies. The detector sensitivities were normalized to their response to 6 MV x rays. The OSLD was bleached between each irradiation. The error bars correspond to one standard deviation of measurement uncertainty.

the radiation with a 21% drop in sensitivity at 120° and 17% drop at 180°. Repeated measurements with the diode at any angle have an uncertainty of 0.3%.

The light-tight case of the OSLD has an areal density of 0.037 g/cm^2. This should make the OSLD an ideal surface detector. To test this hypothesis, an OSLD and a surface diode were compared to the depth-dose response of a parallel-plate ion chamber. These data are shown in Fig. 8. All of the detectors had a maximum response at a depth of 3 cm, which is expected for a 15 MV beam.[40] The OSLD and the diode had small amounts of intrinsic buildup compared to the parallel-plate ion chamber. This is seen as *y*-axis intercepts above that of the parallel-plate ion chamber. The linear portion of the ion chamber depth-dose curve was used to estimate this intrinsic buildup. For the OSLD this was 0.04 g/cm^2, which is very close to what is expected from the areal density of the light-tight case. For the diode the intrinsic buildup was 0.07 g/cm^2, which is less than the 0.11 g/cm^2 stated in the characteristics published by the diode manufacturer.

The energy dependence of the OSLD was determined for the common modes and energies of a linear accelerator used in the clinic as shown in Table I and for a HDR brachytherapy Ir-192 source. The OSLD and the surface diode were placed at the depth of maximum dose for each mode and energy of the linear accelerator and irradiated with 100 cGy. The Ir-192 source and the detectors were separated by 7.1 cm in a stack of solid water and Superflab that was $30 \times 30 \times 30$ cm. These data are shown in Fig. 9. Within measurement uncertainty the OSLD sensitivity was unchanged for typical radiation from a linear accelerator; 6 MV x rays to 20 MeV electrons. Similar results have been reported for the real-time method of measurement.[33] The diode sensitivity is lower by about 6% for the higher energy radiation. For irradiation with Ir-192, average gamma-ray energy of 0.38 MeV, the OSLD sensitivity is elevated by 6% and the diode sensitivity is elevated by 18%. An increased response of $Al_2O_3:C$ material for photons of less than 300 KeV energy has been previously reported.[18]

The linear accelerator delivers dose by giving square pulses of the electron beam at a frequency of a few kilohertz. The dose rate of the accelerator is altered by changing the frequency of the pulses, not the amplitude or the duration of the pulses of the electron beam. For 6 MV x rays on the Siemens KD linear accelerator, the beam current pulse duration was measured to be 2.6 μs. A dose of 1 Gy at source-to-axis distance of 100 cm was found to be delivered with 7200 pulses. This is dose-per-pulse, an instantaneous dose rate, of 1.39×10^{-4} Gy/pulse or 53.4 Gy/s during the pulse. The sensitivity of diodes has been shown[38,41–45] to change when the dose-per-pulse is of this magnitude. This has been found to be a more significant problem for *N*-type diodes.[38,41,42]

The response of the OSLD and the surface diode at different dose-per-pulse values are shown in Fig. 10. The value of dose-per-pulse was varied by making measurements at different distances from the source, with the addition of 1.5 cm thick plates of cerrobend, and placing the detector under the solid collimator jaw of the accelerator. The dose-per-pulse value itself was measured with an ion chamber with sufficient bias voltage to avoid charge-recombination errors. The data in Fig. 10 indicate that the OSLD does not have a change in sensitivity within measurement uncertainty for a dose-per-pulse change of 388-fold. The diode has about a 2.5% increase in sensitivity going from the lowest to highest dose-per-pulse value. No significant difference is seen in the results if the dose-per-pulse was changed by distance or by adding attenuators.

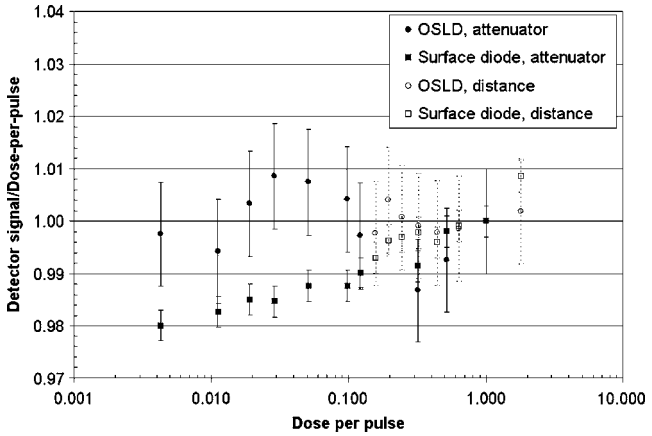

FIG. 10. Dose response of an OSLD and the surface diode as a function of dose-per-pulse of a 6 MV x-ray beam. Exposures were made with a 10 $\times$10 cm field measured at 100 cm from the radiation source of a linear accelerator. The dose-per-pulse value was varied from 1.00 to 0.0043 by adding attenuators. The dose-per-pulse value of 0.0043 was obtained by irradiating the detector with it positioned under a solid-collimator jaw. The dose-per-pulse value was varied from 1.79 to 0.156 by changing the distance to the detector from 75 to 250 cm. The dose-per-pulse values were normalized to the value at a detector-to-source distance of 100 cm without attenuators. The corresponding dose-per-pulse value was 1.39×10^{-4} Gy/pulse, 53.4 Gy/s, 3208 Gy/min. The error bars correspond to one standard deviation of measurement uncertainty.

Since the intent is to use OSLDs for *in vivo* dosimetry, it was of interest to determine if their sensitivity to dose changes with temperature at the time of irradiation. Figure 11 shows how sensitivity to dose of OSLDs and a surface diode depend on the temperature during irradiation. Within experimental uncertainty the OSLD has no temperature dependence. The diode increases in sensitivity by approximately 0.3%/°C.

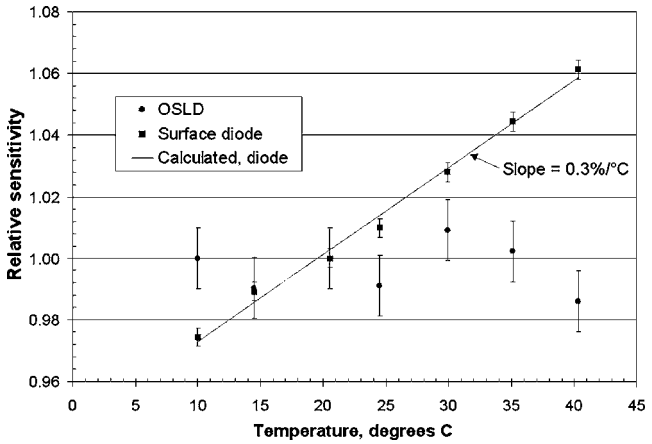

FIG. 11. Sensitivity to dose as a function of the temperature at the time of irradiation. The detectors were irradiated by 100 cGy of 15 MV x rays. Each temperature point was accomplished by adjusting the water bath and allowing 5 min for thermal equilibrium. The temperature of the detectors was established by measuring the forward-bias resistance of the diode immediately before the irradiation. The dose sensitivity of the detectors is normalized to the values measured at 20 °C. The solid line is a calculated temperature sensitivity of 0.3%/°C. The error bars correspond to one standard deviation of measurement uncertainty.

Using the diode as a thermistor, it was taped to the skin surface of a volunteer (the author) to determine what temperature increases might be experienced. A 9.2, 8.6, and 8.3 °C temperature increase was observed for the forearm, cheek, and thigh, respectively. An average temperature increase of 8.5 °C occurs with respect to the ambient temperature at which calibration of detectors would occur. This increase in temperature would result in no change in the OSLD sensitivity to dose but a 2.5% increase for this diode.

IV. DISCUSSION

One of the interesting properties of OSLDs is that they can be read repeatedly with only a 0.05% decrease in signal per reading, as shown in Fig. 2. The OSLD does not have to be totally discharged to obtain significant signals. If the number of reading cycles is recorded, then Eq. (1) can be used to decipher the original signal. This gives one the choice of reading the OSLD and retaining it for future analysis or as a permanent record of the measured dose. The data in Fig. 3 show that after the transient signal decays the signal is stable within 2% for 2.5 days, and it has been reported[15] as stable for 100 days.

The OSLD has a transient signal (Fig. 3) that is a consequence of the filling of low-energy electron traps (7 in Fig. 1) during irradiation and the subsequent spontaneous emptying of these traps in the dark. An 8 min wait after irradiation is the method used in this work to deplete these low-energy traps. A transient signal has been reported[14] that had a decay half-life of 2.5 min, which is longer than the 0.5–0.9 min decay half-time reported in Table III. This difference may be due to different sources of Al_2O_3:C crystals, with different annealing history, which might open electron traps with different energy levels and consequent decay times. Many of the reported OSLD results begin measurements a few milliseconds[29] after the radiation ends or during the radiation.[31] These OSL measurements will include the transient signal of Fig. 3 and may reflect the properties of the low-energy electron traps and the dosimetry trap (4 and 9 in Fig. 1). It is expected that future designs of OSLD readers could incorporate a low-intensity, red light pre-read cycle that could optically empty the low-level traps and not deplete the higher energy dosimetric traps. This would avoid the wait time that is now required before reading the OSLD.

Based on the data shown in Fig. 4, exposure of an OSLD to visible light can be useful. OSLDs can be used repeatedly if they are zeroed, optically annealed, between exposures to radiation. The optical annealing can be accomplished by a 1 min exposure to a tungsten-halogen lamp or many hours in bright room light. If desired, OSLDs can be handled in dim room light, such as found in an accelerator vault, for a few tens of seconds without a significant discharge of their signal as shown in Fig. 6. For *in vivo* measurements of very delicate areas, such as near the eye, it may be preferable to use the OSLD disk out of its light-tight case. The use of dim room light would accommodate this procedure. Alternately, the OSLD disk can be removed from its holder and placed in a light-tight envelope. The author has done this using black

paper from a discarded radiographic-film package. Under dim light the OSLD disk was returned to its plastic reading holder.

A useful modification of the OSLD would be to replace the disk with a 1×1 mm^2 piece of OSL material. The readout holder would have to be altered to accommodate this small OSLD chip. A small OSLD chip would be suitable for measuring very small IMRT segments or stereotactic fields. The OSLD signal is 130 000 counts for 100 cGy for the present disk, which has a 19.6 mm^2 illuminated area. The signal for a 1×1 mm^2 OSLD chip would be approximately $130\,000/19.6=6633$ counts if the low-intensity LED beam was used. The reader also has a high-intensity LED beam with 8.7-fold greater intensity, which would give a signal of $6633\times8.7=57\,704$ counts. This size signal will be adequate for quantitative work.

Dose rate dependence has been reported to be a problem for *N*-type silicon diodes[38,41,42] but not for pre-radiated *P*-type detectors.[42,44] It has since been shown[43,45] that *P*-type silicon diodes do show a dependence on dose-per-pulse, which occurs at much higher accumulated irradiation dose than for *N*-type diodes. Improved *N*-type diodes are now available[39,46] that show dose-per-pulse dependence that is quite similar to what is normally found for *P*-type diodes. The OSLD does not have a change in sensitivity with dose-per-pulse within measurement uncertainty. This means that OSLDs can give accurate dose measurements for a wide range of dose-per-pulse values. These could occur at extended distances for whole body irradiations or total skin electrons, under blocks, under wedges, or under MLC leaves in IMRT beams.

OSLDs can be irradiated, read, and then zeroed many times. The OSLD sensitivity is constant until a dose of about 20 Gy accumulates. Above this dose, the OSLD sensitivity drops about 4% per additional 10 Gy of accumulated dose. It is hypothesized that the OSLD undergoes radiation damage such as that which occurs in diodes[43,44,47,48] with the generation of new traps in the crystal structure. In diodes the change in sensitivity with accumulated dose is much less severe. It has been shown[40,48] that *N*- and *P*-type diodes have a drop in sensitivity of 1.5–2.2% per 1000 Gy of absorbed dose. The average patient treatment delivers about 2.0 Gy per fraction. If one allows a 2% drop in detector sensitivity before a new sensitivity calibration is done, then the frequency of calibration would be every 12 measurements for OSLDs or every 500 measurements for diodes.

The OSLDs responses to absorbed dose are shown in Fig. 6. As can be seen, the OSLDs behave like TLDs (Ref. 2) and exhibit supra-linear response to dose above 300 cGy. It has also been reported that response to dose is linear up to 350 cGy (Ref. 32) and up to 100 Gy.[31] It is not clear why at such high doses[31] the OSL response was not superlinear. The OSLD supra-linear response has been reported previouisly;[11,14,17] the relationship of dose to net OSLD signal counts is given by Eq. (4) for detectors used in this work. The explanation given for the supra-linear response[11,14,17] is that at low dose few deep electron traps (6 in Fig. 1) are filled and they compete with luminescence centers (4 and 9 in Fig. 1) for electrons generated during charge separation. This results in lower amounts of optically stimulated luminescence (processes 9, 11, and 12 in Fig. 1). At higher dose the deep electron traps become filled and more electrons are trapped in the luminescence trap and consequently enhance the optically stimulated luminescence signal.

One method to avoid the radiation damage problem is to use an OSLD once and then discard it. This requires calibration of detectors in a batch versus individually. This method was tested in this work (Table IV) and found to have a measurement uncertainty of 0.9%, which is very close to earlier reported results[32] of 1%. The uncertainty of the multiple use method (Table IV) was found to be 0.6%, which is very close to earlier reported results[32] of 0.7%. The one-use method is convenient and avoids potential radiation damage at normal clinical doses as shown in Fig. 5, but incurs a loss of precision and the extra cost of throwing away detectors after one use.

A very attractive use of OSLDs would be as surface-dose detectors. This can be very helpful when irradiating lesions near the skin surface with electron beams with or without bolus. The intrinsic buildup of the OSLD was found to be 0.04 g/cm^2, which is consistent with its light-tight packaging. Other important characteristics of a surface detector are no dependence on the energy or the angle of incidence of the radiation. This work shows that the OSLD has no angular dependence and no energy dependence in the range of 6 MV x rays to 20 MeV electrons. The OSLD is comparable to TLD chips for measurements of surface dose, but is superior to the surface diode that was tested. The diode had a small dependence on energy (Fig. 9) and a large dependence on the incident angle of the radiation (Fig. 7). Earlier work[29] showed that OSLDs and diodes agreed very closely in measurements of depth dose but no estimates of intrinsic buildup were made.

Within experimental uncertainty the OSLD used here have no dependence on the temperature at the time of irradiation, as shown in Fig. 11. Earlier work[13] reported for temperature at the time of irradiation a temperature coefficient of 0.13%/°C for Al_2O_3:C crystals designated as CZ#60 and 0.02%/°C for crystals designated as TLD-500. It is very likely that these temperature coefficients correspond to the transient decay component of the OSLD decay. In this work this transient decay component has been avoided by the 8 min wait before reading the OSLD. The reading protocol is not specified in this earlier report.[13] Since no mention is made of avoiding a rapid decay transient component, it is presumed that this component has been included in the measured signals.[13] This rapid decay transient component is believed to come from low-energy electron traps (7 in Fig. 1), which will show a positive temperature coefficient in the 10–40 °C range.

The merits of TLDs and OSLDs have been debated in the literature.[49] TLDs have the disadvantage of requiring carefully controlled temperature changes to read the device and complicated recipes for thermally annealing TLDs before subsequent irradiations. OSLDs are read optically which is

simpler to precisely control, and as shown here they can be easily optically annealed. TLDs have an advantage of decades of proven use for radiation measurements, especially *in vivo* dosimetry. OSLDs must be kept in light-tight conditions prior to reading, while TLDS must be handled carefully so that they do not incur surface contamination. Both types of devices can be carefully calibrated and reproducibility of 1.5% can be achieved with TLDs and as shown here better than 1% for OSLDs. The devices themselves are inexpensive, a few dollars each, and they can be reused. The simplicity of the OSLDs reader is reflected in a cost of approximately half that of a TLD reader. Both devices can be used effectively for *in vivo* dosimetry.

V. CONCLUSIONS

OSLDs exhibit high precision and accuracy in measuring dose, are small in size, have no energy dependence, have no dependence on irradiation angle, and can be read long after irradiation. OSLD can substitute for TLD and diodes for *in vivo* dosimetry and routine clinical dose measurements. Because of their very low intrinsic buildup OSLDs are ideal for measuring surface dose. With proper handling OSLDs can be a permanent record of measured dose, they are reusable, the readout process is less than 1 min, and the readout is by optical stimulation versus high temperature so the dosimeter can be made out of inexpensive plastic.

ACKNOWLEDGMENTS

The author would like to thank the Landauer Co. for the loan of OSL dosimeters and the reader. No financial support was given to the author by the Landauer Co. Also, the author would like to thank Dr. Cliff Yahnke for many interesting technical discussions and Gary Beardman for his help in establishing the author's working relationship with Landauer.

[a]Electronic mail: pjursinic@wmcc.org

[1]ICRU Report 24, "Determination of absorbed dose in a patient irradiated by beams of X and Gamma rays in radiotherapy procedures," International Commission on Radiation Units and Measurements, Bethesda, MD, 1976.
[2]F. H. Attix, *Introduction to Radiological Physics and Radiation Dosimetry* (Wiley, New York, 1986), Chap. 14, Integrating Dosimeters, pp. 395–437.
[3]M. Essers and B. J. Mijheer, "*In vivo* dosimetry during external photon beam radiotherapy," Int. J. Radiat. Oncol. Biol. Phys. **43**, 245–259 (1999).
[4]M. Soubra, J. Cygler, and G. Mackay, "Evaluation of a dual bias dual metal oxide-silicon semiconductor field effect transistor detector as radiation detector," Med. Phys. **21**, 567–572 (1994).
[5]D. J. Huntley, D. I. Godfrey-Smith, and M. L. W. Thewalt, "Optical dating of sediments," Nature (London) **313**, 105–107 (1985).
[6]E. J. Rhodes, "Methodological considerations in the optical dating of quartz," Quart. Sci. Rev. **7**, 359–400 (1988).
[7]M. J. Smith, "Optical dating of sediments: initial results from Oxford," Archaeometry **32**, 19–31 (1990).
[8]S. W. S. McKeever, M. S. Akselrod, L. E. Colyott, N. Agersnap-Larsen, J. C. Polf, and V. Whitley, "Characteristics of Al_2O_3 for use in thermally and optically stimulated dosimetry," Radiat. Prot. Dosim. **84**, 163–168 (1999).
[9]R. C. Yoder and M. Salasky, "Optically stimulated luminescence dosimeters—an alternative to radiological monitoring films," in Optical Engineering Midwest 95, Illinois Institute of Technology, 18 May 1995.
[10]L. Bøtter-Jensen and S. W. S. McKeever, "Optically stimulated luminescence dosimetry using natural and synthetic materials," Radiat. Prot. Dosim. **65**, 273–280 (1996).
[11]E. G. Yukihara, V. H. Whitley, J. C. Polf, D. M. Klein, S. W. S. McKeever, and A. E. Akselrod, "The effects of deep trap population on the thermoluminescence of Al_2O_3:C," Radiat. Meas. **37**, 627–638 (2003).
[12]S. Vincellar, G. Molnar, A. Berkane-Krachai, and P. Iacconi, "Influence of thermal quenching on the thermostimulated processes in α-Al_2O_3. Role of F and F^+ centres," Radiat. Prot. Dosim. **100**, 79–82 (2002).
[13]J. M. Edmund and C. E. Andersen, "Temperature dependence of Al_2O_3:C response in medical luminescence dosimetry," Radiat. Meas. **42**, 177–189 (2007).
[14]M. L. Chithambo, "Concerning secondary thermoluminescence peaks in α-Al_2O_3:C," S. Afr. J. Sci. **100**, 524–527 (2004).
[15]L. Bøtter-Jensen, N. Agersnap-Larsen, B. G. Markey, and S. W. S. McKeever, "Al_2O_3:C as a sensitive OSL dosimeter for rapid assessment of environmental photon dose rate," Radiat. Meas. **27**, 295–298 (1997).
[16]B. G. Markey, S. W. S. McKeever, M. S. Akselrod, L. Bøtter-Jensen, N. Agersnap, and L. E. Colyott, "The temperature dependence of optically stimulated luminescence from α-Al_2O_3:C," Radiat. Prot. Dosim. **65**, 185–189 (1996).
[17]E. G. Yukihara, V. H. Whitley, S. W. S. McKeever, A. E. Akselrod, and M. S. Akselrod, "Effects of high-dose irradiation on the optically stimulated luminescence of Al_2O_3:C," Radiat. Meas. **38**, 317–330 (2004).
[18]M. S. Akselrod, V. S. Kortov, D. J. Kravetsky, and V. I. Gotlib, "High sensitivity thermoluminescent anion-defective α-Al_2O_3:C crystal detectors," Radiat. Prot. Dosim. **32**, 15–20 (1990).
[19]M. S. Akselrod, V. S. Kortov, and E. A. Goreleva, "Preparation and properties of α-Al_2O_3:C," Radiat. Prot. Dosimetry **47**, 159–164 (1993).
[20]R. C. Yoder and M. R. Salasky, "A dosimetry system based on delayed optically stimulated luminescence," Health Phys. **72**, S18–S19 (1997).
[21]B. G. Markey, L. E. Colyott, and S. W. S. McKeever, "Time-resolved optically stimulated luminescence from α-Al_2O_3:C," Radiat. Meas. **24**, 457–463 (1995).
[22]M. S. Akselrod and S. W. S. McKeever, "A radiation dosimetry method using pulsed optically stimulated luminescince," Radiat. Prot. Dosim. **81**, 167–175 (1999).
[23]P. Allen and S. W. S. McKeever, "Studies of PTTL and OSL in TLD-400," Radiat. Prot. Dosim. **33**, 19–22 (1990).
[24]R. Gaza, S. W. S. McKeveer, and M. S. Akselrod, "Near-real time radiotherapy dosimetry using optically stimulated luminescence of Al_2O_3:C: Mathematical models and preliminary results," Med. Phys. **32**, 1094–1102 (2005).
[25]S. W. S. McKeever, M. S. Akselrod, and B. G. Markey, "Pulsed optically stimulated luminescence dosimetry using α-Al_2O_3:C," Radiat. Prot. Dosim. **65**, 267–272 (1996).
[26]S. W. S. McKeever and M. S. Akselrod, "Radiation dosimetry using pulsed optically stimulated luminescence of using α-Al_2O_3:C," Radiat. Prot. Dosim. **84**, 317–320 (1999).
[27]M. S. Akselrod, N. Agersnap-Larsen, V. Whitley, and S. W. S. McKeever, "Thermal quenching of F-center luminescence in Al_2O_3:C," J. Appl. Phys. **84**, 3364–3373 (1998).
[28]M. S. Akselrod, L. Bøtter-Jensen, and S. W. S. McKeever, "Optically stimulated luminescence and its use in medical dosimetry," Radiat. Meas. **41**, S78–S99 (2007).
[29]M. C. Aznar, C. E. Andersen, L. Bøtter-Jensen, S. Å. J. Bäck, S. Mattsson, F. Kjaer-Kristoffersen, and J. Medin, "Real-time optical-fiber luminescence dosimetry for radiotherapy: Physical characteristics and application to photon beams," Phys. Med. Biol. **49**, 1655–1669 (2004).
[30]R. Gaza, S. W. S. McKeveer, M. S. Akselrod, A. Akselrod, T. Underwood, C. Yoder, C. E. Andersen, M. C. Aznar, C. J. Marckmann, and L. Bøtter-Jensen, "A fiber dosimetry method based on OSL from Al_2O_3:C: For radiotherapy applications," Radiat. Meas. **38**, 809–812 (2004).
[31]J. C. Polf, E. G. Yukihara, M. S. Akselrod, and S. W. S. McKeever, "Real-time luminescence from Al_2O_3:C fiber dosimeters," Radiat. Meas. **38**, 227–240 (2004).
[32]E. G. Yukihara, E. M. Yosimura, T. D. Lindstrom, S. Ahmad, K. K. Taylor, and G. Mardirossian, "High-precision dosimetry for radiotherapy using optically stimulated luminescence technique and thin Al_2O_3:C dosimeters," Phys. Med. Biol. **50**, 5619–5628 (2005).
[33]C. E. Andersen, M. C. Aznar, L. Bøtter-Jensen, S. Å. J. Bäck, S. Mattsson, and J. Medin, "Development of optical fibre luminescence techniques for real-time in-vivo dosimetry in radiatherapy," in IAEA-CN-96–118, International Symposium on Standards and Codes of Practice in

Medical Radiation Dosimetry, Vienna, 2002.
[34]P. R. Almond, P. J. Biggs, B. M. Coursey, W. F. Hanson, M. S. Huq, R. Nath, and D. W. O. Rogers, "AAPM's TG-51 protocol for clinical reference dosimetry of high-energy photon and electron beams," Med. Phys. **26**, 1847–1870 (1999).
[35]R. Nath, L. L. Anderson, G. Luxton, K. A. Weaver, J. F. Williamson, and A. S. Meigooni, "Dosimetry of interstitial brachytherapy sources: Recommendations of the AAPM radiation therapy committee Task Group No. 43," Med. Phys. **22**, 209–234 (1995).
[36]D. R. White, "Tissue substitutes in experimental radiation physics," Med. Phys. **5**, 467–479 (1978).
[37]P. A. Jursinic, "Changes in incident photon fluence of 6 and 18 MV x-rays caused by blocks and block trays," Med. Phys. **26**, 2092–2098 (1999).
[38]P. A. Jursinic, "Implementation of an *in vivo* diode dosimetry program and changes in diode characteristics over a 4-year clinical history," Med. Phys. **28**, 1718–1726 (2001).
[39]P. A. Jursinic and B. E. Nelms, "A 2-D diode array and analysis software for verification of intensity modulated radiation therapy delivery," Med. Phys. **30**, 870–879 (2003).
[40]T. J. Jordan, "Megavoltage x-ray beams: 2–50 MV," Br. J. Radiol. Suppl. **25**, 62–109 (1996).
[41]E. Grusell and G. Rikner, "Radiation damage induced dose rate nonlinearity in an *N*-type silicon detector," Acta Radiol. Oncol. **23**, 465–469 (1984).
[42]G. Rikner and E. Grusell, "General specifications for silicon semiconductors for use in radiation dosimetry," Phys. Med. Biol. **32**, 1109–1117 (1987).
[43]J. Van Dam, G. Leunens, and A. Dutreix, "Correlation between temperature and dose rate dependence of semiconductor response; influence of accumulated dose," Radiother. Oncol. **19**, 345–351 (1990).
[44]E. Grusell and G. Rikner, "Linearity with dose rate of low resistivity *p*-type silicon semiconductor detectors," Phys. Med. Biol. **38**, 785–792 (1993).
[45]D. Wilkins, X. A. Li, J. Cygler, and L. Gerig, "L. "The effect of dose rate dependence of *p*-type silicon detectors on linac relative dosimetry," Med. Phys. **24**, 879–881 (1997).
[46]J. Shi, W. E. Simon, and T. C. Zhu, "Modeling the instantaneous dose rate dependence of radiation diode detectors," Med. Phys. **30**, 2509–2519 (2003).
[47]J. Shi, "Characteristics of the Si diode as a radiation detector for the application of in-vivo dosimetry," Master's thesis, Florida Institute of Technology, May (1985).
[48]A. S. Saini, T. C. Zhu, J. R. Palta, and J. Shi, "A comparison of commercially available *N*- and *P*-type Si diode detectors," Med. Phys. **23**, 1071 (1996).
[49]S. W. S. McKeever and M. Moscovitch, "On the advantages and disadvantages of optically stimulated luminescence dosimetry and thermoluminescence dosimetry," Radiat. Prot. Dosim. **104**, 263–270 (2003).